Supplementary information

Silver Nano-needles: Focused Optical Field Induced Solution Synthesis and Application on Remote-Excitation Nanofocusing SERS

*Pan Li, Deng Pan, Longkun Yang, Hong Wei, Shuli He, Hongxing Xu, and Zhipeng Li**

Dr. P. Li, Dr. L. K. Yang, Prof. S. He and Prof. Z. P. Li
The Beijing Key Laboratory for Nano-Photonics and Nano-Structure (NPNS), Center for Condensed Matter Physics, Department of Physics, Capital Normal University, Beijing 100048, P.R. China
E-mail: zpli@cnu.edu.cn
Dr. D. Pan
School of Physics and Technology, Wuhan University, Wuhan 430072, P. R. China
Prof. H. Wei
Beijing National Laboratory for Condensed Matter Physics, Institute of Physics Chinese Academy of Sciences, University of Physics Chinese Academy of Sciences, Collaborative Innovation Center of Quantum Matter, Beijing 100190, P. R. China
Prof. H. X. Xu
School of Physics and Technology, Wuhan University, Wuhan 430072, P. R. China
The Institute for Advanced Studies, Wuhan University, Wuhan 430072, P. R. China
Division of Solid State Physics/The Nanometer Structure Consortium, Lund University, Box 118, S-22100, Lund, Sweden

Experimental Section

Experimental Setup for Nano-Needles Synthesis: A drip of a reaction mixture was placed in a cell consisting of a slide of Indium tin oxide (ITO) glass and a cover glass, and mounted onto an inverted dark-field optical microscope. The reaction mixture was prepared by mixing aqueous solutions of silver nitrate and sodium citrate with the respective concentrations of 5 and 7 mM in a volume ratio of 1:1. A 980 nm continuous wave laser with the power of 120 mW was focused on the ITO glass through an objective with 100× magnification (NA = 0.7). This resulted in a spot size of about 10 nm in diameter. After 1 min irradiation, the products on ITO glass were washed with deionized water and dried for SEM measurements.

Characterizing the growth process and morphology of silver nano-needles: The optical dark-field images of the synthesis process were recorded by a CCD detector (DVC, 10 frames per second), where the infrared laser was removed from the image by adding a short-pass edge filter in the front of detector. SEM and EBSD measurements were carried out under JSM-7001F (JEOL) working at voltage 15 kV and 30 kV, respectively. The TEM images and SAED patterns were recorded on a Tecnai F30 microscope operating at 300 kV.

Mapping the surface plasmons propagation in silver nano-needles: The surface plasmons propagation were launched by focusing a laser beam (633 nm) through an oil immersed objective (100×/NA=1.3) on the thicker end of the needle. The emission from the other end of the needle was collected by the same objective and the optical image was recorded by the CCD mounted on the microscope. To visualize the near-field distributions of surface plasmons, the needles were first covered with a layer of aluminum oxide (Al2O3) with a thickness of 10 nm by atomic layer deposition to prevent quenching of the QDs fluorescence. Then, CdSe/ZnS core/shell quantum dots (QDs, Invitrogen, SKU# Q21321MP, diluted 200 times) were spin-coated with the speed 400 r/min onto the needles. QDs adjacent to the needle can be excited by evanescent fields of propagating plasmons that are launched by focusing the laser at the thicker end of the needle. These luminescent QDs act as" reporters" of the local field at every point along the entire structure. After filtering the laser light, the fluorescence image was recorded by the CCD detector.

Plasmons imaging of silver nano-needle with s-SNOM: The plasmons near field imaging of silver nano-needles were measured using s-SNOM (Neaspec GmbH) base on interferometric pseudoheterodyne detection. The probes were commercially available metallized AFM probes with an apex radius about 10 nm (Nanoworld). The tip height was modulated at a frequency

of approximately 285 kHz with an amplitude of 45-65 nm. The optical signals were obtained from the third harmonic interferometric pseudo-heterodyne signal. The plasmons were launched and imaged by raster scanning the nano-needle with the probe under excitation of 633 nm laser.

Simulations: Electromagnetic calculations were based on a finite element method (COMSOL Multiphysics). The model is a needle with a pentagonal cross-section on an ITO substrate covered by a layer of 10 nm Al2O3 surrounded by oil (Fig. S9a). The field distributions and effective refractive indices of eigenmodes were obtained using the mode solver in COMSOL. The dielectric permittivity of silver is taken from Johnson and Christy (Phys. Rev. B 6, 4370, 1972). The refractive indices used for ITO, Al2O3 and oil are 1.78, 1.76 and 1.53, respectively.

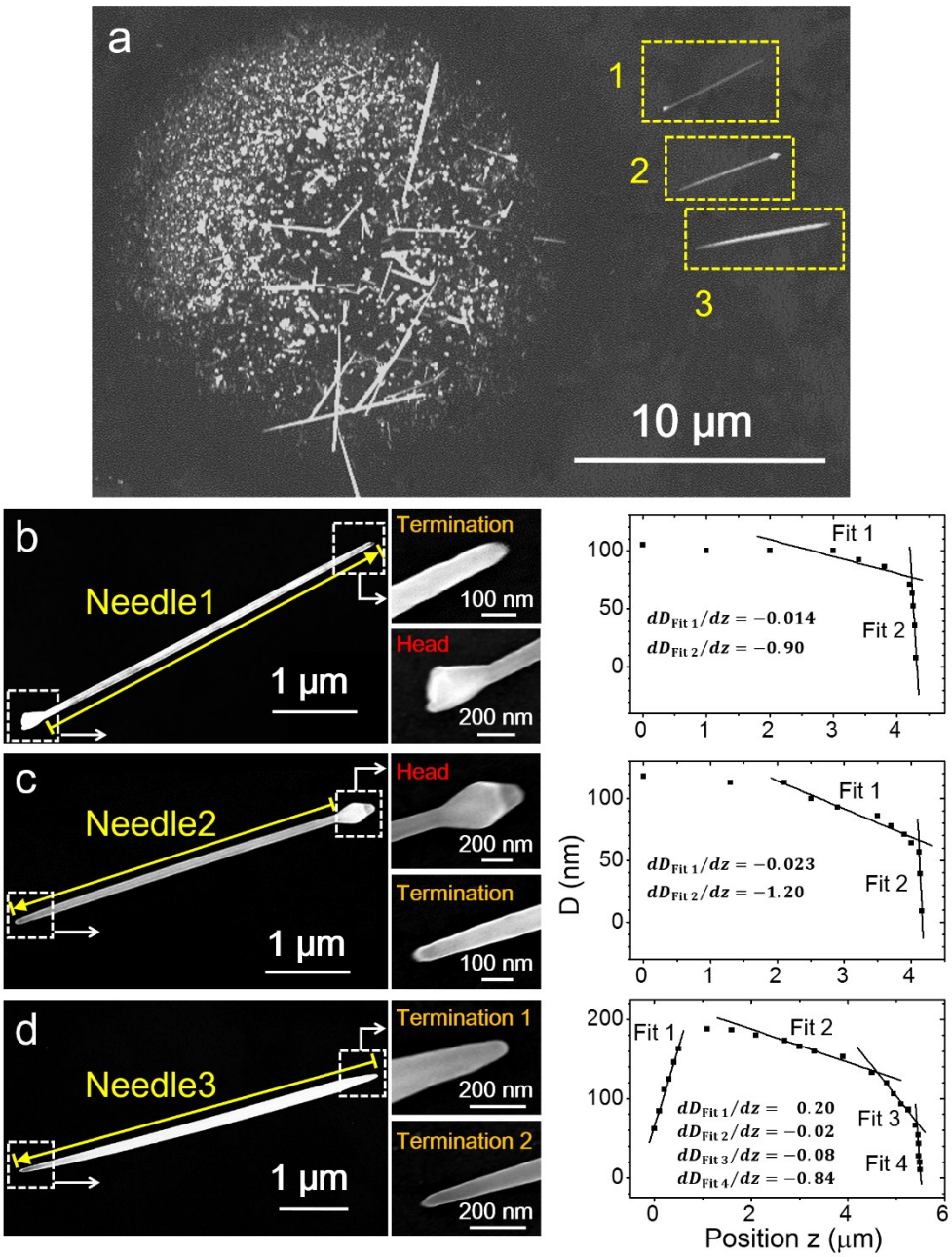

Fig. S1. Synthesized silver nano-needles with different morphologies. (a) SEM image of the products after laser irradiation. **(b)-(d)** Close-up views of the nano-needles (1-3) indicated by the yellow squares in (a). The insets show zoomed views of the respective sharp terminations and/or big heads. In the right columns, the corresponding needle diameters *D* as functions of the positions *z* from the start to the end point along the yellow lines in (b)-(d) are given. The black lines are linear fits for different parts of the needles.

Discription: in the first 27 s illumination, numerous silver nanoparticles formed. After that, a rod-like particle began to grow, as tracked by the yellow arrow in Fig. S2a (I). Within three seconds, the particle fast elongated along the radial direction of the laser spot (II and III) with the growth rate about 1.2 μm/s. At 31 s, the needle was abruptly ejected out of the laser spot with a speed of ~17 μm/s, and deposited on the substrate several micrometers from its initial position (IV). The process between 23 and 32 s is presented in Movie S2. Fig. S2b and S2c show SEM images of the synthesized nano-needles. It is found that the needle points to the beam center with its thin end.

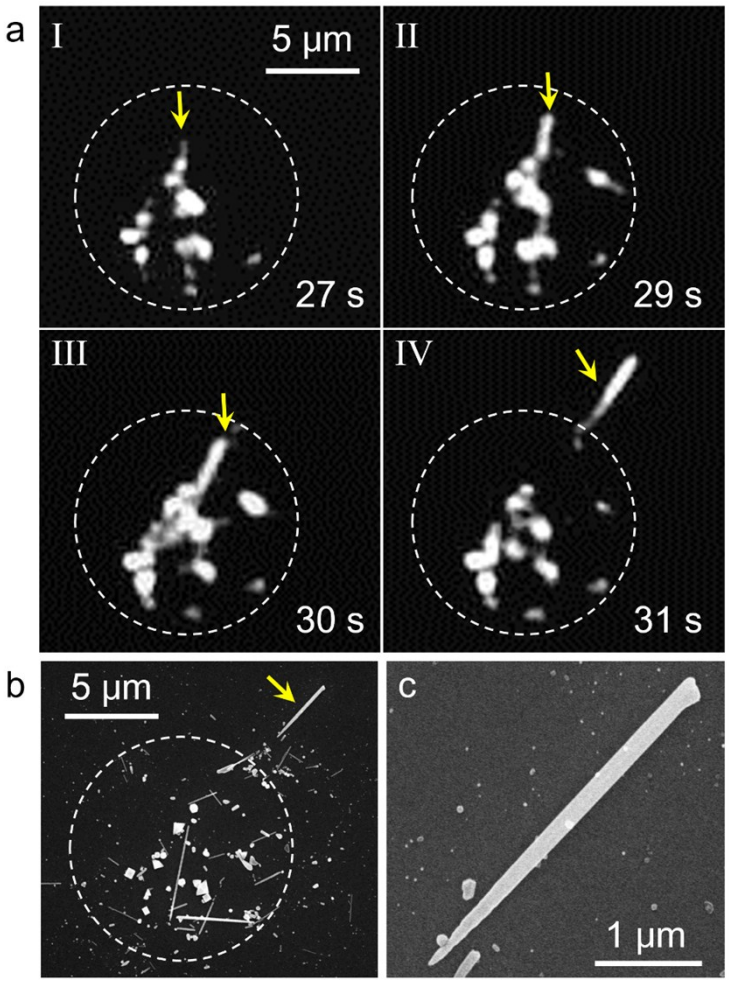

Fig. S2. Growth process of silver nano-needles. (a) Dark-field images of the products after 27 s (I), 29 s (II), 30 s (III) and 31 s (IV) of laser irradiation, which are extracted from the Movie S2. The white circle indicates the size of the laser beam and the yellow arrow tracks one needle in different growth stages. **(b)** SEM image of the products in the area shown in (a) after 32 s irradiation. **(c)** Close-up view of the nano-needle indicated by the yellow arrow in (b). Its length is 3.7 μm and diameter attenuating from 170 nm to 10 nm.

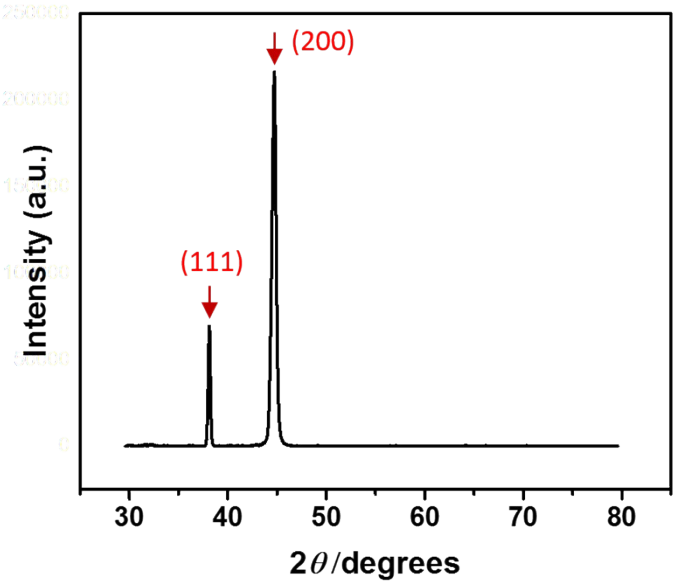

Fig. S3. **X-ray diffraction pattern of the Ag NNs sample.** The NNs were synthesized on glass with illumination time 120 s. The pattern was measured by a Bruker D8 diffractometer with integral time 10 hours. The result shows that the sample have fcc crystal structure.

Discription: the diffraction patterns with nice contrast demonstrate that the NN is well crystallized in an fcc structure, thus exhibiting an ultra-smooth surface. The [110] direction of the unit cell is parallel to the longitudinal axis of the wire. It was also found that Kikuchi patterns from different positions of the wire can give mirror symmetric fcc unit cells, which implies that the NN possesses a multiply twin structure with the [110] as the common direction.

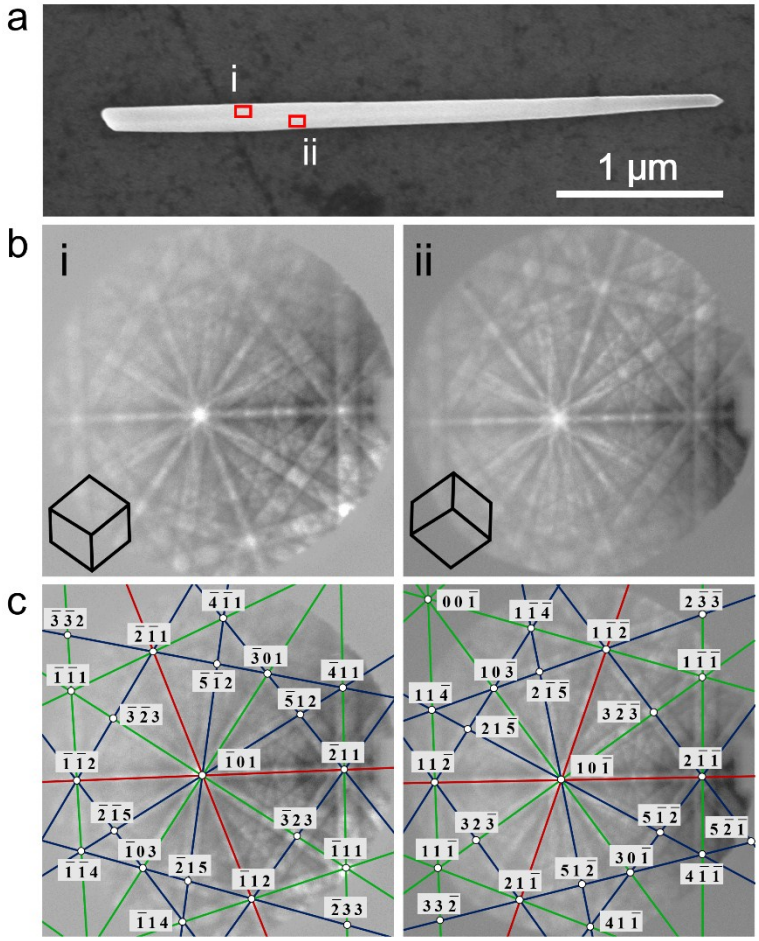

Fig. S4. Electron backscatter diffraction measurements on a silver NN. (a) SEM image of a NN with length of 3.7 μm, diameters of 160 and 70 nm at each end, and a tip size of ~8 nm. **(b)** Measured Kikuchi patterns from the positions i and ii indicated in (a). The corresponding unit cells with matching orientations are shown in the lower left corners. **(c)** Kikuchi patterns with indexation.

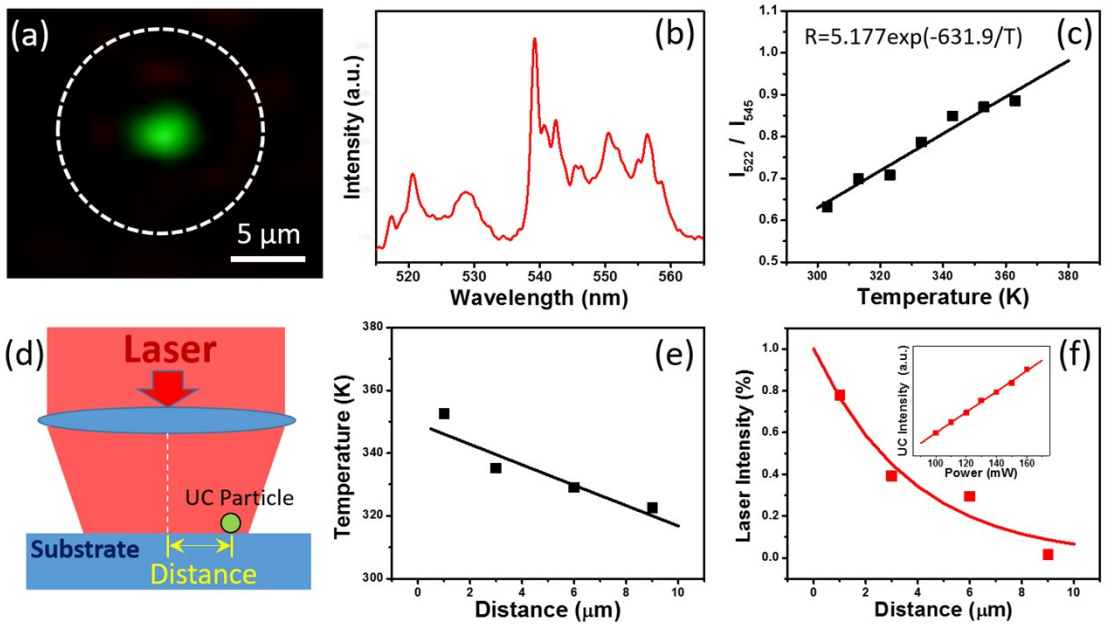

Fig. S5. Temperature and light intensity sensing based on Er-Mo:$Yb_3Al_5O_{12}$ upconvertion (UC) luminescence. (a) Luminescence image of UC particles aggregate (diameter around 700 nm) at the excitation of 980 nm laser. The white circle indicates the photoexcitation area of laser spot. **(b)** A typical spectrum of the UC luminescence. Due to the thermal excitation between the $^2H_{11\backslash 2}$ and $^4S_{3\backslash 2}$ levels, the intensity ratio of luminescence from $^2H_{11\backslash 2} \rightarrow {}^4I_{15\backslash 2}$ and $^4S_{3\backslash 2} \rightarrow {}^4I_{15\backslash 2}$ can be used as an effective temperature indicator. **(c)** The Luminescence intensity ratio (R) of the UC particles at 522 and 546 nm as a function of the environment temperature. The fitting curve (line) follow the relation R=5.177exp(-631.9/T). The max error of the fitting is ±8 K. **(d)** Scheme of the temperature and light intensity sensing. By changing the distance between the particle and the center of the laser spot, the luminescence at different positions can be detected. **(e)** Temperature as a function of the distance to the center of laser spot, extracted by the fitting equation in (c). To mimic the circumstance of the photochemical experiment, the cell is filled with water, and the laser power is 120 mW. It shows that the laser irradiation causes a 30 K difference between the spot center and edge. **(f)** The decay of the relative laser intensity from spot center to edge, which is obtained by the linear relation between luminescence and laser intensity. The inset shows the luminescence intensity as a function of laser power.

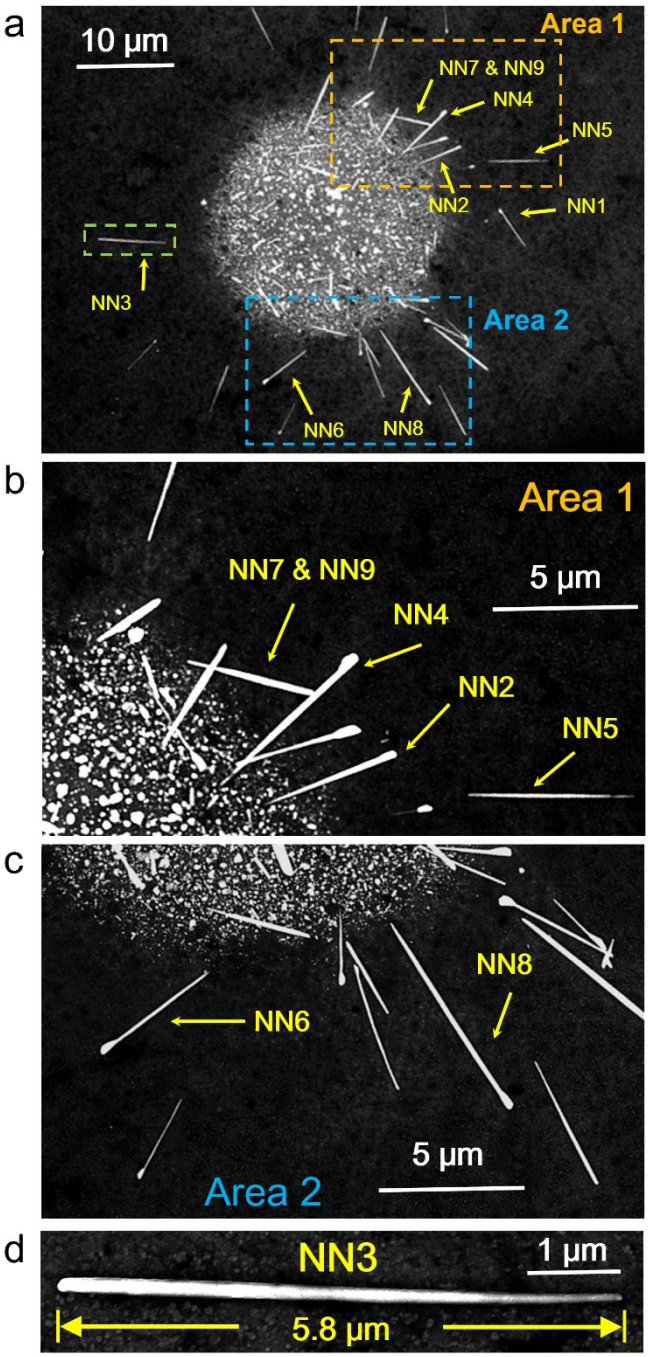

Fig. S6. The SEM image of the final products for the synthesis process in Supplementary Movie 1. (a) SEM image of the products after 110 s irradiation. About 33 needles can been found in the image. The synthesis process during 32-59 s was captured by CCD camera and shown in Supplementary movie 1, where we marked the trajectory of nine needles (1-9) denoted in (a) by yellow arrows. **(b, c)** Zoom-in images of the area 1 and area 2 in (a). Needle 7 and 9 are finally merged together. **(d)** SEM image of needle 3 with the length 5.8 μm. The diameters of each end are 157 nm and 62 nm, respectively. NN stands for nano-needle.

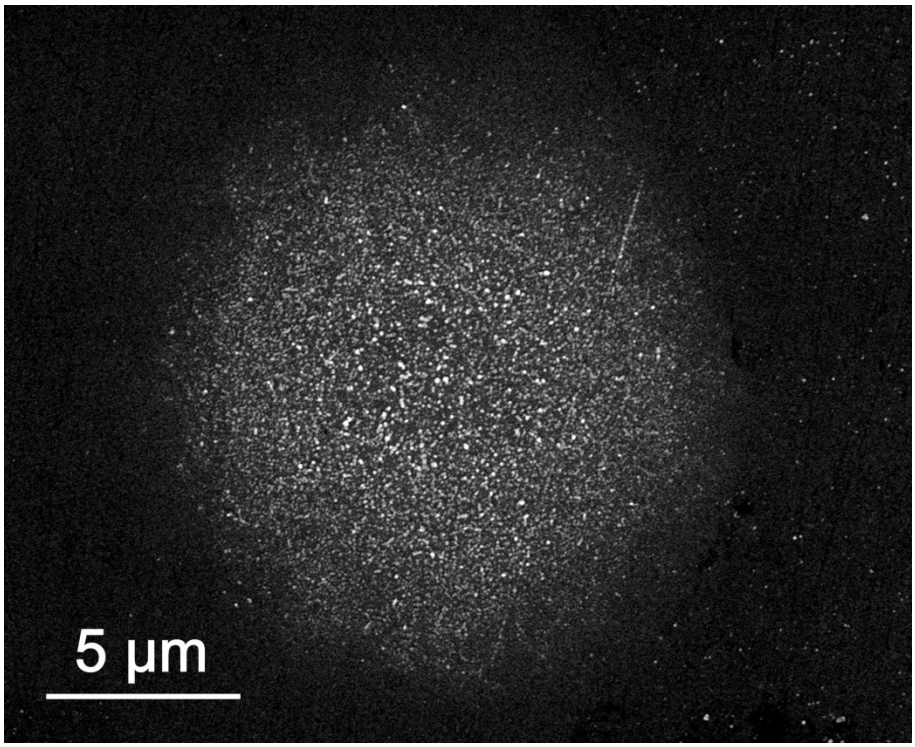

Fig. S7. NNs yield below the threshold of laser power. SEM image of the products after 60 s of laser irradiation with a lower excitation power of ~90 mW, while maintaining the same silver nitrate and sodium citrate concentrations as used previously (silver nitrate and sodium citrate with concentrations of 5 mM and 7 mM are mixed in a volume ratio of 1:1).

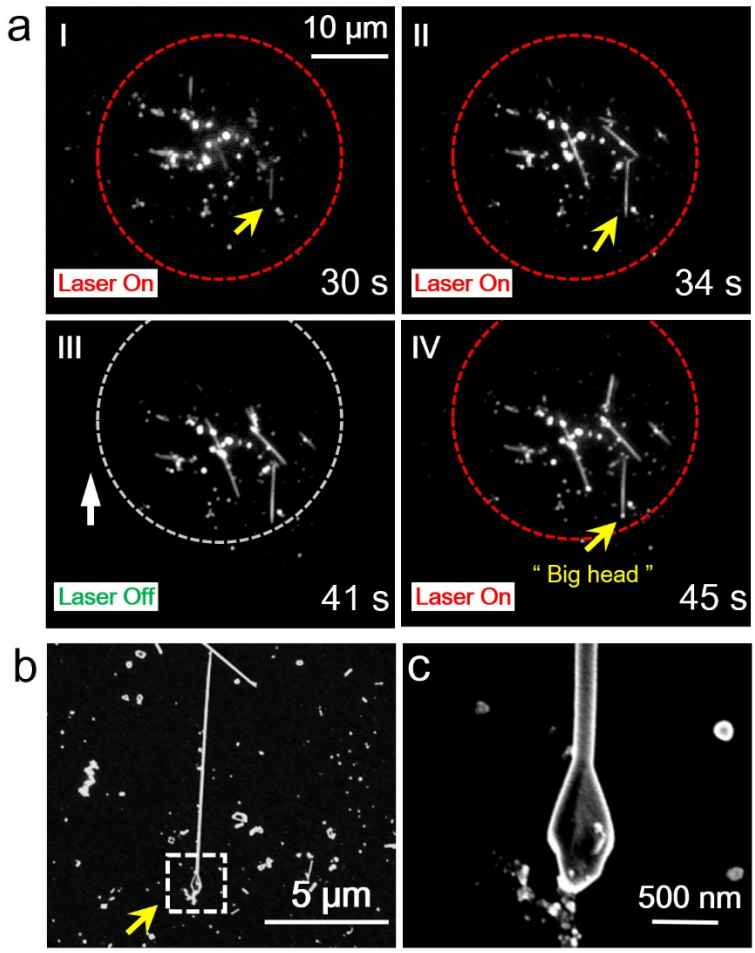

Fig. S8. Active control the photochemical synthesis by moving the relative position of focused laser spot. (a) Dark-field optical images of the products at different growth stages: 30 s (I), 34 s (II), 41 s (III) and 45 s (IV). One needle in different growth stages is tracked by a yellow arrow. The illumination was maintained in the first 34 s of the synthesis. After that, turning off the laser during the 35 s and 41 s and moving the tracked needle to the edge of laser spot which is indicated by the red and white circles. And then, the laser was turned on at 42 s and triggered the needle growth again. From the dark-field image, it was found that a new "big head" was formed in the end of tracked needle. All panels (I-IV) share the same scale bar 10 μm. **(b)** SEM image of the tracked nano-needle. Its length is 10 μm and diameter attenuates from 120 nm to 57 nm. **(c)** Close-up view of the needle head.

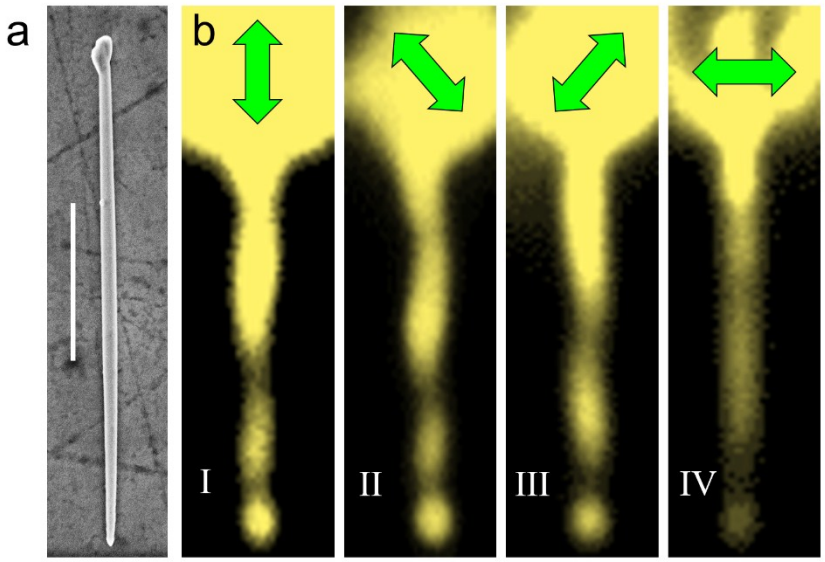

Fig. S9. Chiral plasmons in NN. (a) SEM image of a silver NN with a length of 6.5 μm and diameters of 210 nm and 85 nm at each end. The scale bar corresponds to a length of 2 μm. **(b)** QDs emission images of the nano-needle under the excitation at the thicker end with different polarizations as indicated by the green arrows.

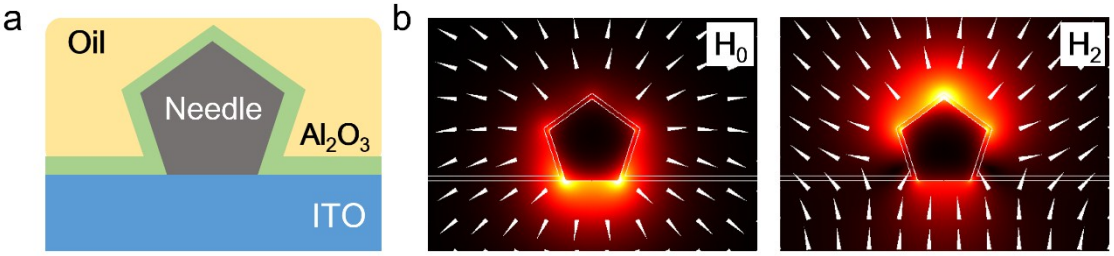

Fig. S10. Modelled plasmon modes in silver NN. (a) Schematic cross-section of the modelled NN on ITO substrate covered by a layer of 10 nm Al_2O_3. **(b)** Calculated electric field distributions of the two plasmon modes H_0 and H_2 for a needle with diameter of 200 nm under the excitation of 633 nm. White arrows mark the directions of electric field.

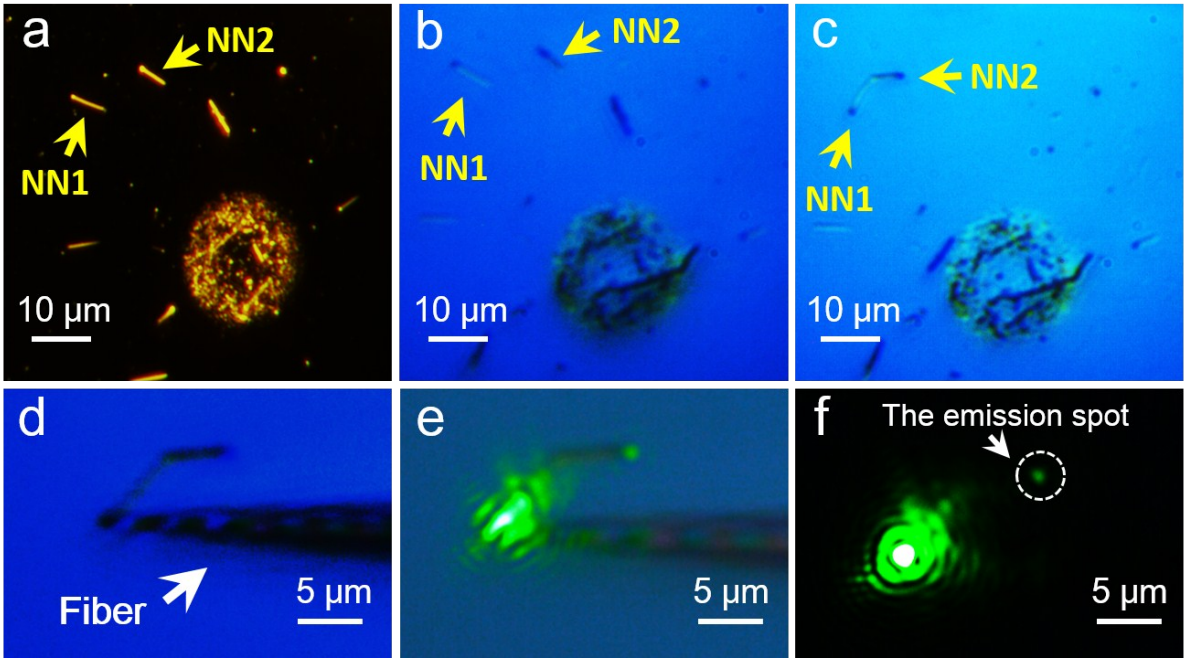

Fig. S11. Manipulate NNs by optical fiber to construct nanowaveguide connections. (a) Optical dark-field image of synthesized NNs. **(b)** Optical bright field image of the needles. **(c)** The optical image of an assembled nano-needle connection. With oil hydraulic micromanipulator (step resolution 2 μm), the NNs can be pushed by a tapered optical fiber and form arbitrary connections. **(d)-(f)** Launch SPPs propagation on the assembled NN connection via a tapered optical fiber. The wavelength of the excitation light is 532 nm. The clear emission spot from the assembled nanowaveguide connection in (f) demonstrates that the synthesized NN can be promising build block for on-chip nanophotonic circuit.

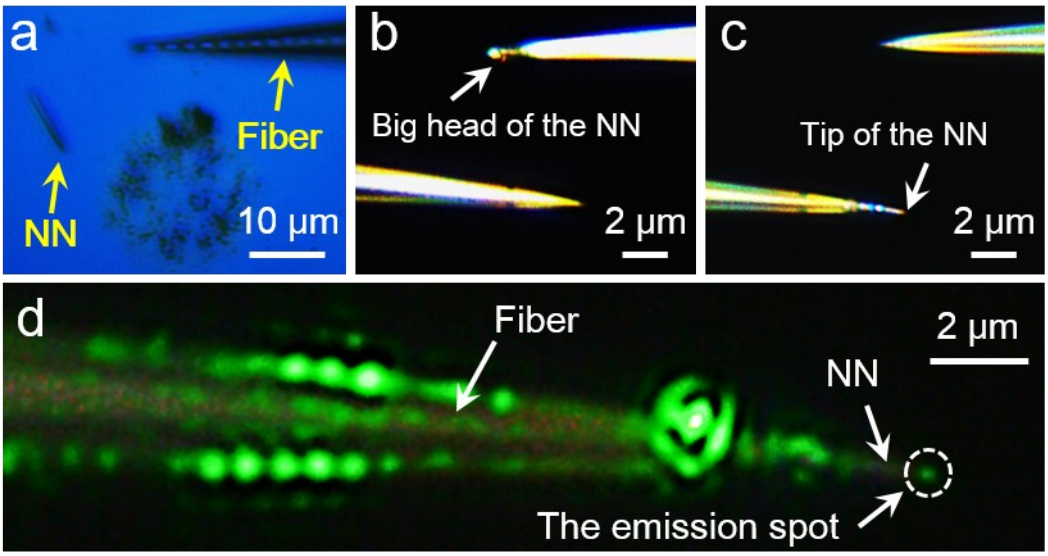

Fig. S12. Pick up and install a NN onto tapered optical fiber for scanning probe. (a) Optical bright field image of the synthesized needle (~8 μm in length) and a tapered optical fiber controlled by oil hydraulic micromanipulator. **(b)-(c)** Pick up and install the synthesized needle onto a tapered optical fiber. With the oil hydraulic micromanipulator, the upper fiber is first pressed on the NN and then lifted up. The NN can be attached on the fiber via van der Waals force and picked up from the substrate, as shown in (b). The picked up NN is then transferred to the lower tapered fiber coating with UV-curing optical adhesives, as shown in (c). **(d)** Launch SPPs in nano-needle via optical fiber by "end-fired" configuration. A bright emission spot at the apex of the NN is clearly observed. The wavelength of the excitation light is 532 nm.

Movies Description:

Movie S1: Movements of NN in the laser spot. Thermophoresis and convection lead to ejection (e.g. NN2, NN3, NN4), flip-over (e.g. NN1) and backflow (e.g. NN9) of the nano-needles. To facilitate the observation, the movie is played at half of the original speed. The SEM images of these nano-needles are presented in the Fig. S6.

Movie S2: Dynamic growth process of the silver NN shown in the Fig. S2. Recorded from 23 to 32 s during the laser irradiation. For clarity, the movie is shown at half of the original speed.

Movie S3: Active control the morphology of silver NNs shown in the Fig. S8. Recorded from 30 to 45 s during the synthesis. For clarity, the movie is shown at half of the original speed.